The Cooperative Relation between Temper Embrittlement and Hydrogen Embrittlement in a High Strength Steel

KENICHIRO YOSHINO AND C. J. McMAHON, JR.

A sample plate of HY 130 steel (5 pct Ni-0.5 pct Cr-0.5 pct Mo-0.1 pct V-0.1 pct C) was found to be quite susceptible to temper embrittlement. Step-cooling produced a shift in transition temperature of 583 K (310°C). In the step-cooled condition the plane strain stress intensity threshold for crack growth in 0.1 N H_2SO_4 was about 22 $MNm^{-3/2}$ (20 ksi $\sqrt{in.}$) and the fracture mode was intergranular, whereas in the unembrittled condition the threshold for a 1.27 cm ($\frac{1}{2}$ in.) plate (not fully plane strain) was around 104.5 $MNm^{-3/2}$ (95 ksi $\sqrt{in.}$) and the fracture mode was mixed cleavage and microvoid coalescence. The interaction between the impurity-induced and the hydrogen embrittlement is discussed in terms of Oriani's theory of hydrogen embrittlement.

FOR a number of years it has been recognized that quenched and tempered alloy steels have a tendency to fracture along prior austenite grain boundaries under conditions of stress corrosion or hydrogen embrittlement.[1] Since this mode of fracture is also associated with impurity-induced grain boundary weakening, as in temper embrittlement and "500°F" embrittlement, it is natural to ask whether these two types of embrittlement may act in a cooperative manner.

The literature on this subject is quite sparse. Cabral *et al.*[2] tested smooth bars of a quenched and tempered 3 pct Ni, 0.6 pct Cr, 0.1 pct Mo, 0.11 pct Cu, 0.3 pct C steel by static loading in tension in 0.1 N H_2SO_4 and found that the threshold for hydrogen-induced fracture* was lowered when the steel was given a prior treatment of 773 K (500°C) for 48 h. This effect was accompanied by a shift from transgranular fracture to fracture along prior austenite grain boundaries. More recently, the exhaustive analysis of the failure of several forged turbine discs of 3.25 pct Cr-0.6 pct Mo steel at the Hinckley Point power station in England has led to the conclusions[3] that the discs had been temper embrittled during manufacture and that the failure was due to the slow growth of an intergranular crack under the influence of condensate trapped in a round keyway, the latter acting as a stress concentrator.

*It is generally concluded that environment-assisted cracking of high strength steels in a hydrogen-producing environment can be attributed to hydrogen embrittlement.

To gain more information about this effect we have investigated the behavior of a new, high strength, naval pressure vessel steel, HY 130, with respect to its susceptibility to temper embrittlement and the influence of such embrittlement on its resistance to crack propagation in a hydrogen-producing environment.

KENICHIRO YOSHINO, Formerly Research Fellow, Department of Metallurgy and Materials Science, University of Pennsylvania is now, Assistant Manager, Kamaishi Works, Nippon Steel Corporation, Kamaishi, Iwate, Japan. C. J. McMAHON, JR., is Associate Professor, Department of Metallurgy and Materials Science, University of Pennsylvania, Philadelphia, Pa. 19174.

Manuscript submitted February 27, 1973.

EXPERIMENTAL PROCEDURE

The sample of HY 130 steel was supplied through the courtesy of the United States Steel Corporation in the form of a cross-rolled one-inch plate. The chemical composition and typical mechanical properties, as determined by U. S. Steel, are shown in Table I.

The response to temper embrittlement was studied by determination of the ductile-brittle transition temperature of 0.63 cm ($\frac{1}{4}$ in.) round bars circumferentially notched and tested in cantilever bending over a range of temperatures, a method originated by Low *et al.*[4] and used by our group in previous work.[5] Temperatures were obtained by immersion in baths of liquid nitrogen, isopentane, or silicone oil, and fracture energies were obtained from the areas under the load-deflection curves taken from an Instron chart. Test bars were heat treated in evacuated capsules by austenitizing at either 1473 K (1200°C) or 1093 K (820°C), quenching in iced brine, and tempering at 898 K (625°C) for 2 h. Some specimens were embrittled by step cooling in the usual way,[4,5] and others were isothermally embrittled at 753 K (480°C) for 25, 100, and 200 h. Notching was done after all heat treatment was completed. The mechanical properties after this step cooling treatment were: yield strength, 848 MN/m^2 (123 ksi); tensile strength, 931 MN/m^2 (135 ksi); Rc hardness, 32.

The resistance to environmental cracking was evaluated by testing edge-notched cantilever bend specimens, shown in Fig. 1, in the manner of Brown and coworkers.[6] The bars were heat treated as above, except that a dynamic vacuum and plain water quenching were used. After heat treating and notching, the bars were fatigue-cracked for a distance of 1 mm (0.040 in.) below the notch at the rate of about 0.025 mm (0.001 in.) per 1000 cycles, as recommended for sharp cracks.[7] The fatigue cracking was done at room temperature for unembrittled specimens and at 523 K (250°C) for embrittled (step-cooled) specimens. This was to insure that cracking was stable and transgranular in both cases. The plane of the fatigue crack was perpendicular to the rolling plane.

The environment used was 0.1 N H_2SO_4 containing

Table I. Chemical Composition and Mechanical Properties of HY 130*

Heat No.	Plate No.	Ladle Analysis (wt pct) C	Mn	P	S	Si	Ni	Cr	Mo	V
5P 2004	0116856 A-1	0.11	0.88	0.003	0.006	0.35	4.95	0.53	0.50	0.08

	Tensile Properties†						Notch Toughness	
	Yield Strength (0.2 pct Offset)		Tensile Strength		Elongation in	Reduction	Charpy V-Notch Energy Absorption at 273 K	
Orientation	ksi	MN/m^2	ksi	MN/m^2	5.08 cm (2 in.) pct	of Area pct	Ft-lb	M,
Longitudinal	139	959	151	1042	20.0	64.2	78	105.7
Transverse	130	897	150	1035	20.0	61.1	68	92.2

*Determined by U.S. Steel Corporation Research Laboratory.
†Austenitized at 1088 K (1500°F), water quenched, tempered at 898 K (1160°F) for 1 h, water quenched.

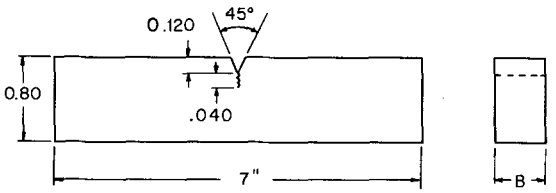

Fig. 1—Notched and precracked bar used for hydrogen embrittlement testing.

5 mg arsenic pentoxide per liter of solution. It was held around the notched portion of the test bar in a Plexiglas chamber attached by GE RTV sealant. The load was applied after the environment was inserted in the chamber. The statically applied loads were such as to give stress intensities at various levels below the value K_c needed to break the bar in the same test arrangement in air. The K calibration used was that of Kies *et al*;[8]

$$K = \frac{4.12M(\alpha^{-3} - \alpha^3)^{1/2}}{BD^{3/2}}$$

where M is the bending moment at the notch, B and D are the thickness and depth of the specimen, respectively, and $\alpha = 1 - a/D$, where a is the total length of the notch plus fatigue crack.

Attempts to monitor crack growth optically were prevented by the tendency for the cracks to propagate faster in the central portion of the unembrittled bars. However, the progress of cracking could be monitored (but not measured) by means of an LVDT placed on the cantilever beam at a distance 12.7 cm (5 in.) from the notch. Time to failure was measured automatically by a microswitch and timer arrangement.

RESULTS

The large susceptibility of this heat of HY 130 steel to temper embrittlement by step cooling is demonstrated in Fig. 2, which shows the results for austenitic grain sizes of 0.01 and 0.03 mm, obtained by austenitization at 1093 K (820°C) and 1473 K (1200°C), respectively. In these experiments the test method of Low *et al.*[4] was used, and the deflection to produce an audible brittle crack is plotted against test temperature. The transition temperature shifts, which have been

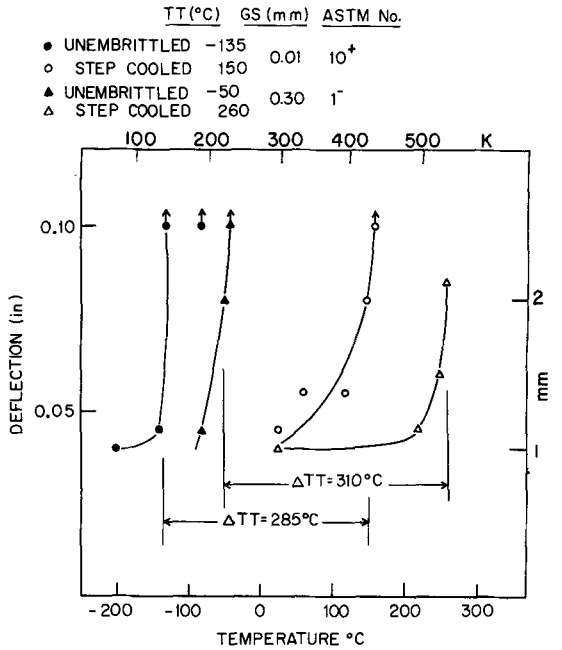

Fig. 2—Shifts in transition temperature due to step cooling embrittlement.

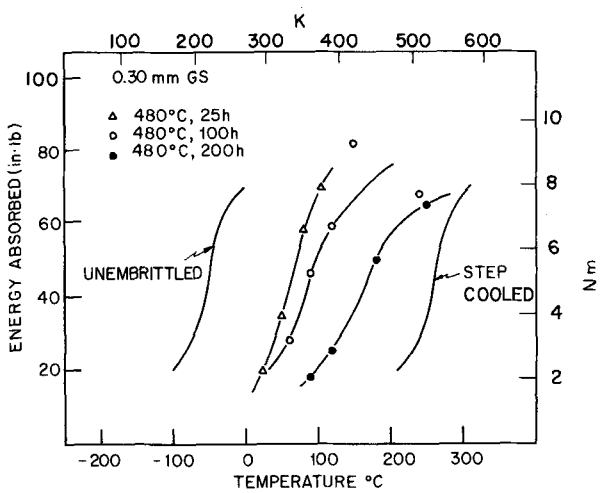

Fig. 3—Shifts in transition temperature due to isothermal embrittlement at 753 K (480°C).

found to correlate approximately with those obtained in Charpy tests, show that in the coarse grained condition the steel is slightly more susceptible, as expected.

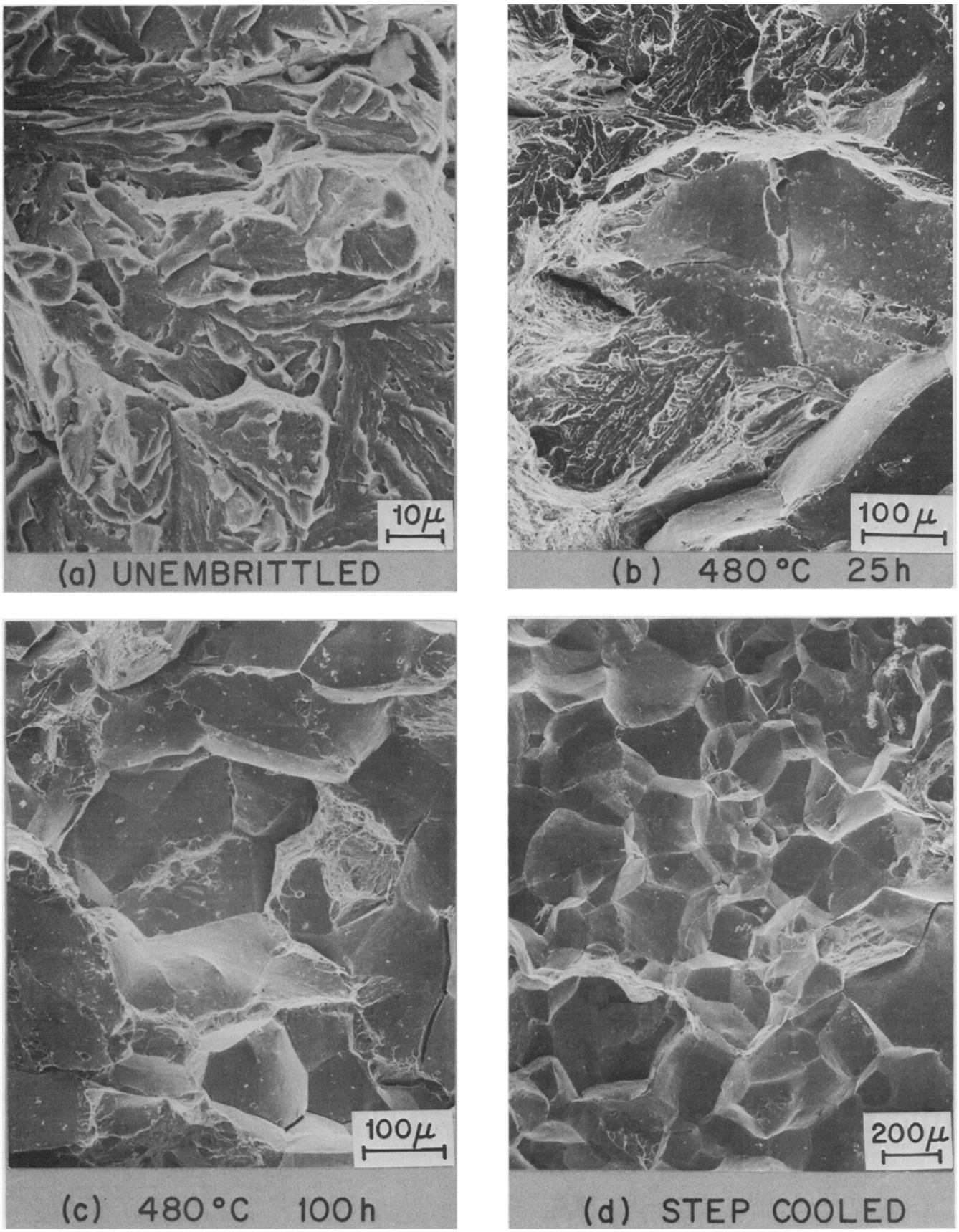

Fig. 4—Fracture surfaces of specimens broken below the transition temperature showing increasing amounts of intergranular embrittlement in the order: (*a*) unembrittled, 193 K (– 80°C) fracture; (*b*) isothermally embrittled, 753 K (480°C), 25 h, 293 K (20°C) fracture; (*c*) isothermally embrittled, 753 K (480°C), 100 h, 363 K (90°C) fracture; (*d*) step cooled, 293 K (20°C) fracture.

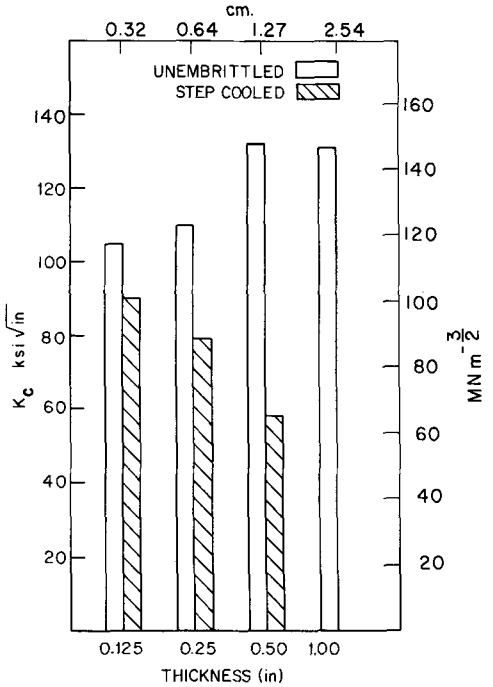

Fig. 5—Values of K_I ($=K_Q$) for unstable crack extension in air tests on precracked cantilever bars (cf. Fig. 1) of various thicknesses in the unembrittled and step cooled conditions. Valid K_{IC} values obtained for the step cooled 1.27 cm ($\frac{1}{2}$ in.) thick bar.

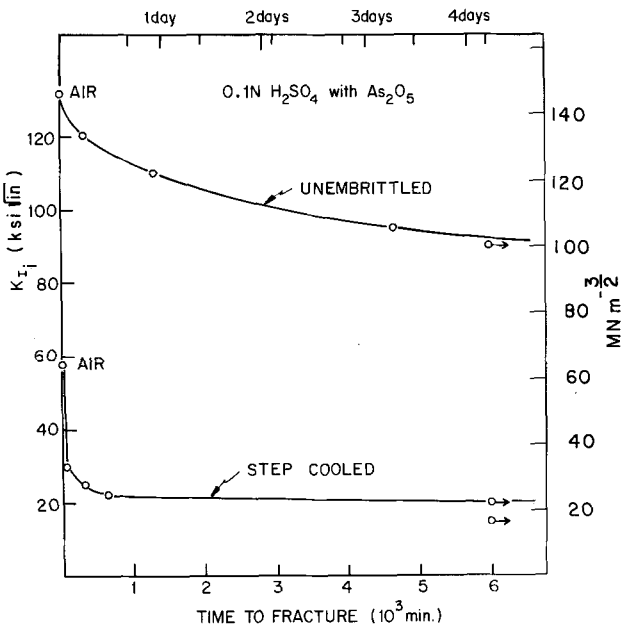

Fig. 6—Initial values of K_I in hydrogen embrittlement tests on precracked cantilever bars (cf. Fig. 1), statically loaded, plotted against time to fracture.

This coarse grained condition was employed throughout the rest of this work.

When isothermal embrittlement at the arbitrarily selected temperature of 753 K (480°C) was carried out, the transition temperature shifted upward with time, as shown in Fig. 3, but it reached only 443 K (170°C) in 200 h, as compared with 533 K (260°C) transition temperature produced by the 168 h step-cooling treatment. The progress of embrittlement can be seen in the fractographs shown in Fig. 4 from specimens fractured on the low temperature side of the ductile-brittle

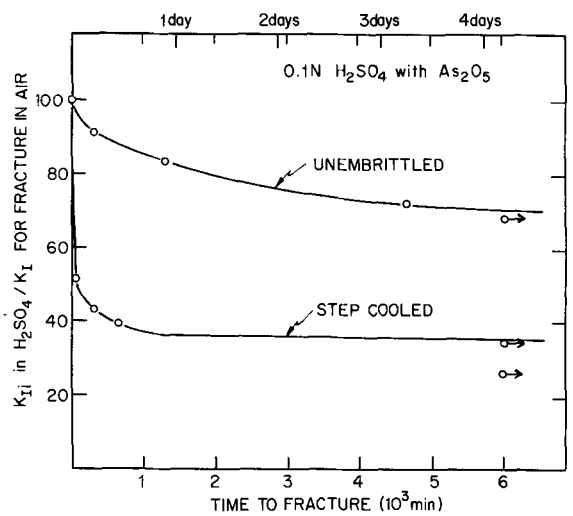

Fig. 7—Data of Fig. 6 plotted in terms of the K_C values in air.

transitions. The specimens range from the unembrittled condition, through the isothermally embrittled conditions at 25 and 100 h, to the step-cooled condition.

The results of the fracture toughness tests in cantilever bending conducted in air on the specimen depicted by Fig. 1 in the unembrittled and step-cooled conditions are shown in Fig. 5. None of these tests are valid plane strain tests (yielding a true K_{I_C}), except the 1.27 cm ($\frac{1}{2}$ in.) thick, step cooled specimen. The unembrittled specimens all exhibited shear lips; however, none of the step-cooled specimens did. The step-cooled specimens fractured intergranularly. The 1.27 cm ($\frac{1}{2}$ in.) thickness was selected for environmental testing.

When the precracked cantilever bend specimens were tested in the 0.1 N H_2SO_4 in the unembrittled and the step-cooled conditions, it was found that the impurity-induced embrittlement has a profound effect on the resistance to crack growth in this hydrogen-producing environment. The initial K_I vales are plotted against time to fracture in Fig. 6, and the same data are shown normalized to the K_C values in air in Fig. 7. It can be seen that the K threshold for hydrogen embrittlement is lowered from about 104.5 MNm$^{-3/2}$ (95 ksi$\sqrt{in.}$) in the unembrittled case to about 22 MNm$^{-3/2}$ (20 ksi$\sqrt{in.}$) for the step-cooled condition. The unembrittled threshold would presumably be lowered if thicker specimens had been used to develop a fully constrained plane strain fracture, but the step-cooled specimen almost meets the K_{I_C} requirement of 1.40 cm (0.55 in.) thickness for a K_C of 63.8 MNm$^{-3/2}$ (58 ksi$\sqrt{in.}$) and a yield stress of 848 MN/m^2 (123 ksi), and the threshold of 22 MNm$^{-3/2}$ (20 ksi$\sqrt{in.}$) therefore is probably the minimum that would be observed for this condition of embrittlement.

The fracture mode in the H_2SO_4 for the unembrittled case is shown in Fig. 8. At the onset of slow crack growth some intergranular fracture could be observed (Fig. 8(*a*)), but this soon shifted to a mixture of cleavage and microvoid coalescence (Fig. 8(*b*)) and then to fully cleavage in the fast-fracture region (Fig. 8(*c*)). It can be seen from Fig. 9 that the hydrogen-produced crack propagated faster in the central portion where the triaxial stress state was more fully developed.

For the embrittled specimens in the H_2SO_4 the hydrogen-produced fracture propagated along a more or less straight front (Fig. 10) and was intergranular

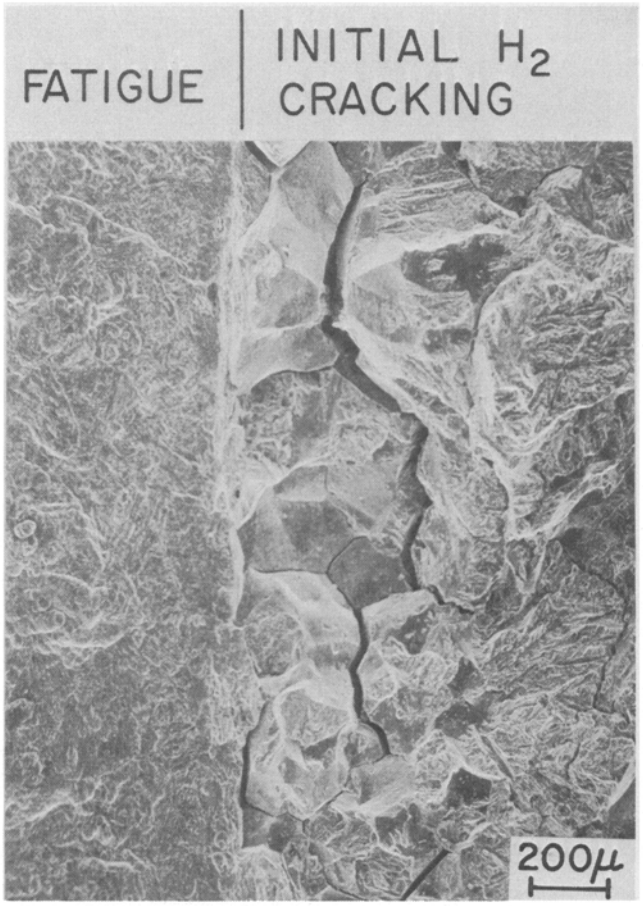

(a)

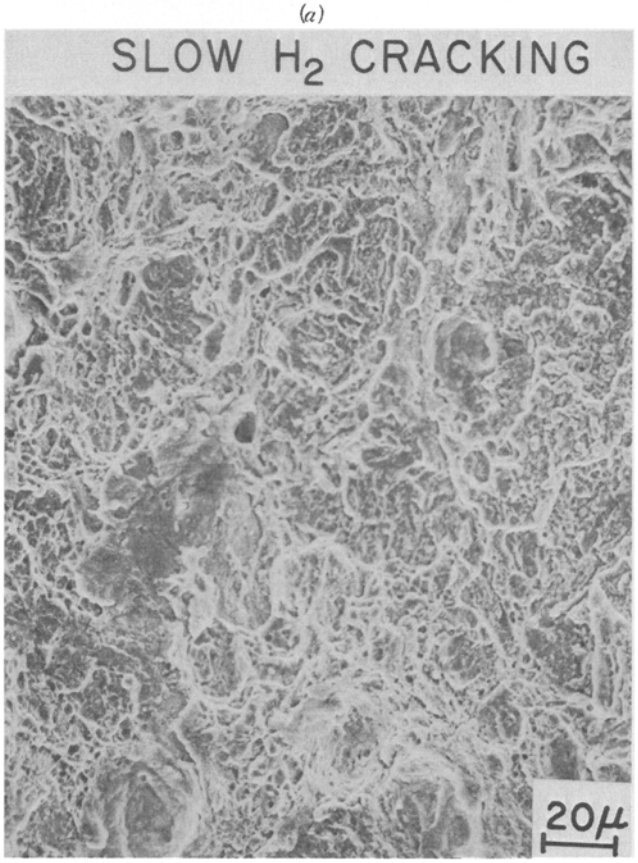

(b)

Fig. 8—Fracture surfaces of unembrittled specimens tested as in Fig. 6 showing: (*a*) initiation, (*b*) slow hydrogen cracking, and (*c*) fast cracking regions.

(c)

from the point of initiation (Fig. 11(*a*)), through the slow growth region (Fig. 11(*b*) and (*c*)), and the fast growth region.

DISCUSSION

The results of this work show that HY 130 steel can be remarkably susceptible to temper embrittlement. In fact, the 583 K (310°C) shift in transition temperature due to step cooling appears to be by far the largest such shift ever reported in a commercially produced alloy steel. When it is recalled that the present steel was investigated at a yield strength level of 848 MN/m^2 (123 ksi), that this steel is designed for yield stress levels up to 1035 MN/m^2 (150 ksi), and that temper embrittlement susceptibility is often found to increase with hardness level, then it must be concluded that this phenomenon deserves further study in this steel and that great care should be taken in the heat treatment of thick sections to be used in critical applications. For example, one would like to know more about the effects of postweld stress relief in such applications as submarine pressure hulls.

Since we do not yet fully understand how the various alloying elements interact with the various embrittling elements to establish temper embrittlement susceptibility, it is not possible at this point to say why this steel should be so susceptible. However, it contains significant amounts of Cr and Mn which are known to enhance embrittlement by P,[4,9] and the combination of Ni and Cr has been shown to enhance embrittlement by Sb, Sn, and As.[4] A temper embrittled specimen was broken in ultrahigh vacuum at 110 K and the intergranular fracture surface was analyzed by Auger electron spectroscopy.[10] It was found that the segregated ele-

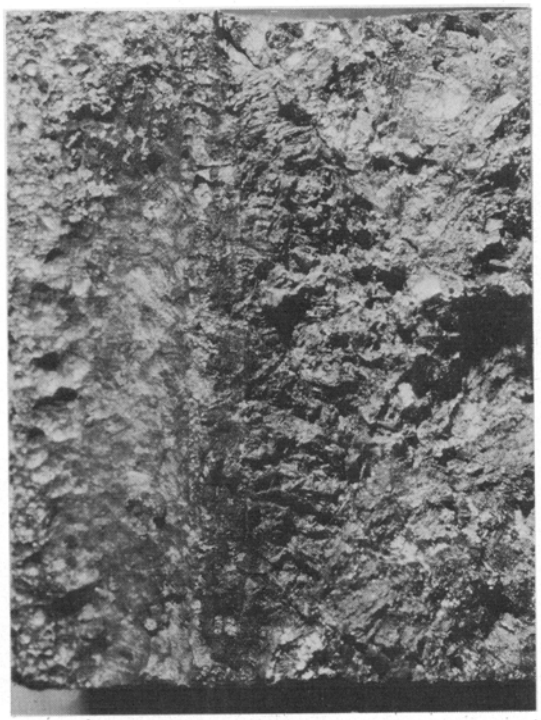

(a)

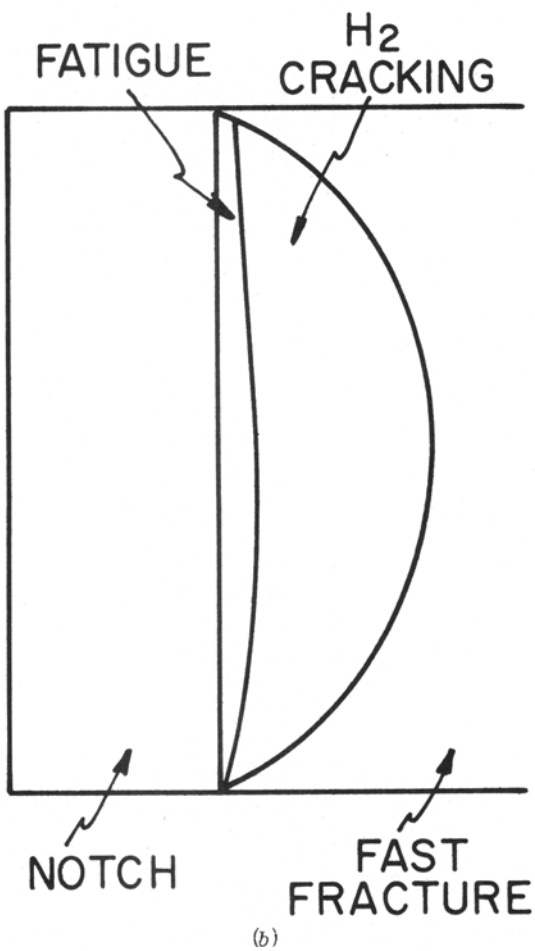

(b)

Fig. 9—Fracture surface of unembrittled specimen tested as in in Fig. 6 showing more extensive hydrogen cracking in the central portion of the test bar.

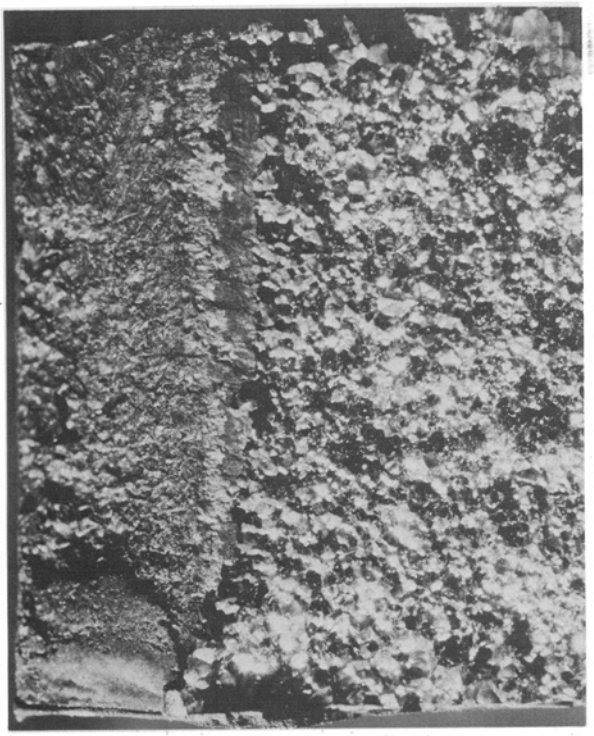

(a)

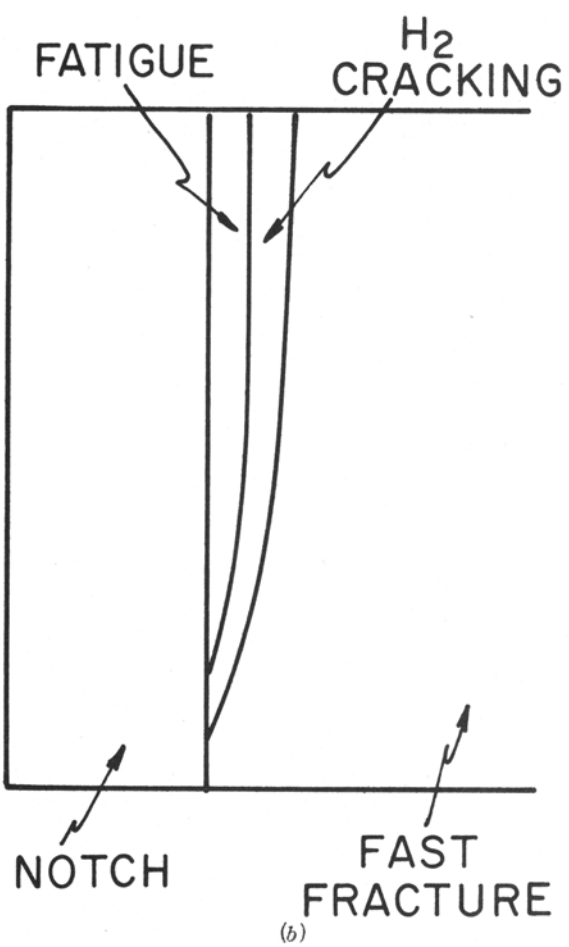

(b)

Fig. 10—Fracture surface of step cooled specimen tested as in Fig. 6 showing uniform rate of hydrogen cracking through the thickness. Compare with Fig. 9.

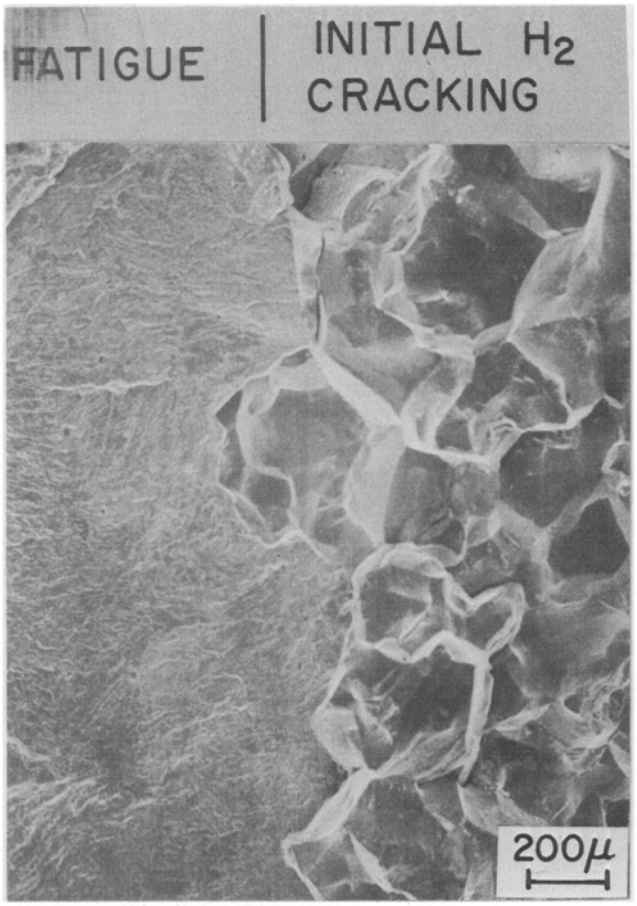

(a)

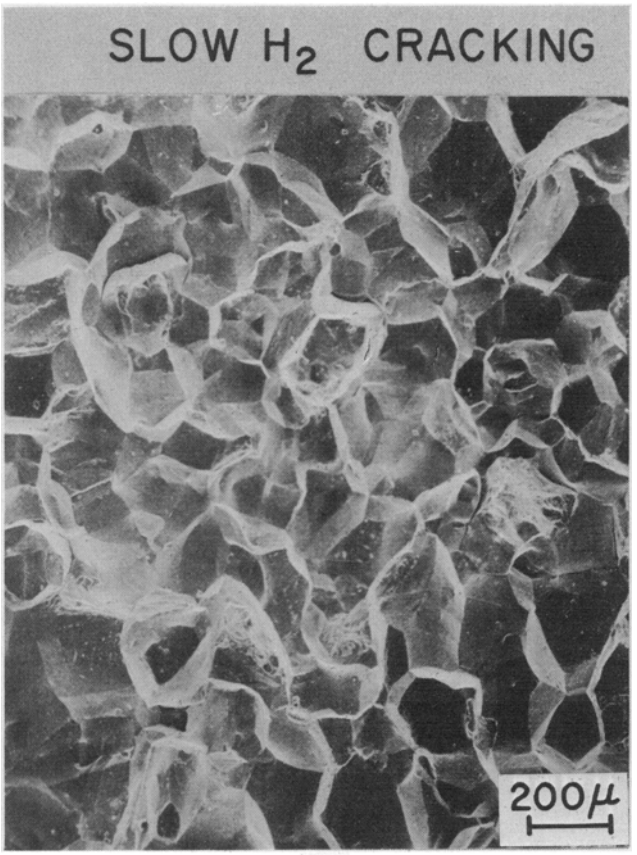

(b)

(c)

Fig. 11—Fracture surfaces of step cooled specimens tested as in Fig. 6 showing (*a*) initiation region and (*b*) and (*c*) slow hydrogen cracking regions.

ments (presumably responsible for the reduction of grain boundary cohesion) were P, Mn, and Si.

The cooperative effect of the impurity-induced embrittlement and the hydrogen-producing environment can be understood qualitatively in a straightforward manner by extending the recent theory of Oriani.[11] Under the triaxial constraint at the tip of a sharp crack in a thick body a large component of stress normal to the crack plane can build up without relaxation by plastic flow. In addition, this region of hydrostatic tension expands the iron lattice and thus lowers the chemical potential of dissolved hydrogen in the vicinity of the crack tip,[12] thereby creating a sink for hydrogen. There are compelling reasons to postulate that, as the hydrogen concentration builds up, the maximum cohesive force of iron is decreased.[11] The latter can be depicted schematically by a lowering of the binding energy curve for the alloyed iron, Fig. 12(*a*). In the unembrittled case the resultant mixture of cleavage and microvoid coalescence signifies that hydrogen-induced cleavage cracks form ahead of the main crack and are joined by plastic failure.

For the embrittled state a large body of experimental evidence leads us to make a similar postulate that the maximum cohesive force along prior austenite grain boundaries is lowered by the buildup of segregated impurities, as can be schematically illustrated in Fig. 12(*b*). From the present results we conclude that the presence of collected hydrogen can lower this cohesive strength still more, so that crack growth can occur along these grain boundaries at very low values of stress intensity, hence with very small attendant plastic zones and, therefore, small amounts of ab-

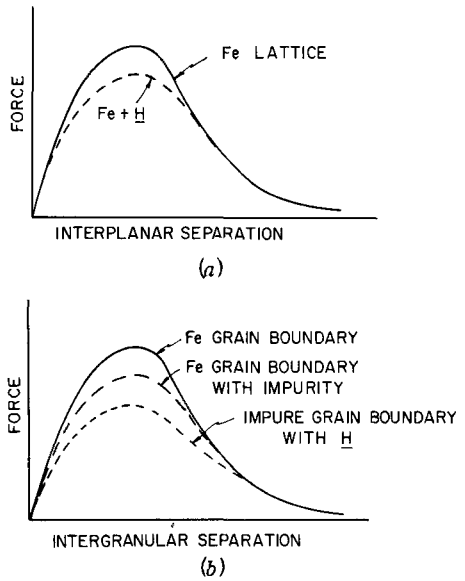

Fig. 12—(*a*) Schematic plot of cohesive force vs separation of atomic planes in an iron lattice in the absence of hydrogen (solid curve) and with a certain concentration of hydrogen present in the vicinity of the crack tip (dashed curve), after Oriani, Ref. 11. (*b*) Similar plot to 12(*a*) showing the proposed additive effect from the superposition of the impurity effect and the hydrogen effect.

sorbed energy. When considered in this way, the additive effect seems quite natural, and these observations are thus consistent with Oriani's analysis, which puts the main emphasis on the lowering of the maximum cohesive force by collected hydrogen.

It is hardly necessary to point out that this tendency for hydrogen embrittlement and impurity-induced embrittlement to act together in an additive fashion presents possibilities of failures of large structures at very low stresses. Hence, we suggest that this effect deserves increased attention in the near future.

CONCLUSIONS

1) Samples from a commercially produced heat of HY 130 steel have been found to be remarkably susceptible to temper embrittlement; a 583 K (310°C) increase in transition temperature resulted from step-cooling.

2) In the step-cooled (embrittled) condition the steel was found to be highly susceptible to intergranular crack growth in a hydrogen-producing environment (0.1 N H_2SO_4), whereas the same steel in the unembrittled condition is much less sensitive to hydrogen.

3) This cooperative action of hydrogen and cohesion-lowering impurities can be understood in terms of the Oriani theory of hydrogen embrittlement.

ACKNOWLEDGMENTS

This work was supported by the Advanced Research Projects Agency of the Department of Defense through the LRSM at the University of Pennsylvania. It formed part of an M.S. thesis submitted to the Department of Metallurgy and Materials Science in 1972 by K. Yoshino, who received financial support for this study from Nippon Steel Corporation.

REFERENCES

1. *Electron Fractography Handbook, Supplement II,* AFML TR 64416, March, 1968, Section B.
2. U. Q. Cabral, A. Hache, and A. Constant: *C. R. Acad. Sci., Paris,* 1965, vol. 260, pp. 6887-90.
3. D. Kalderon: *Inst. Mech. Eng., London,* 1972, vol. 186, pp. 341-77.
4. J. R. Low, D. F. Stein, A. M. Turkalo, and R. P. Laforce: *Trans. TMS-AIME,* 1968, vol. 242, p. 14.
5. B. J. Schulz and C. J. McMahon, Jr.: in *Temper Embrittlement of Alloy Steels,* ASTM STP 499, pp. 104-35, ASTM 1972.
6. B. F. Brown: *Mater. Res. Stand.,* ASTM 1966, vol. 6, p. 129.
7. W. F. Brown, Jr. and J. E. Scrawley: *Plane Strain Crack Toughness of High Strength Metallic Materials,* ASTM STP 410, ASTM 1972.
8. J. A. Kies, H. L. Smith, H. E. Romine, and H. Bernstein: in *Fracture Toughness Testing and Its Applications,* ASTM STP 381, ASTM, Phila., 1965.
9. C. J. McMahon, Jr.: in *Temper Embrittlement in Steel,* ASTM STP 407, pp. 127-67, ASTM, Phila., 1968.
10. K. Yoshino, H. C. Feng, and C. J. McMahon, Jr.: *Proc. Internl. Conf. on Stress Corrosion Cracking and Hydrogen Embrittlement of Iron Base Alloys,* Unieux-Firminy, France, June 1973.
11. R. A. Oriani: *Ber. Bunsenges. Phys. Chem.,* vol. 76, 1972, pp. 848-57; also *Proc. Internl. Conf. on Stress Corrosion Cracking and Hydrogen Embrittlement of Iron Base Alloys,* Unieux-Firminy, France, June 1973.
12. J. C. M. Li, R. A. Oriani, and L. S. Darken: *Z. Phys. Chem.,* (N. F.) vol. 49, 1966, p. 271.